Halo polarization profiles and sampled ice crystals: observations and interpretation

Gunther P. Können, Herman R. A. Wessels, and Jaap Tinbergen

Simultaneous two-wavelength polarization and radiance distributions have been obtained for 22° parhelia in four Antarctic ice-crystal swarms that extended to ground level. Samples of crystals that produced these parhelia were collected and replicated. The wavelength dependence of the width of the halo polarization peak agrees with Fraunhofer diffraction theory, indicating that the broadening of the halos is caused primarily by diffraction. However, the observed broadening is much more than predicted from the size distribution of the replicated crystals. From one halo display to the other, the ratio of observed/predicted broadening is erratic, suggesting size-dependent collection efficiency in the sampling. This would imply that, for South Pole conditions, halo polarimetry (or even photometry) is a more reliable method for crystal size determination than actual sampling. It also implies that shapes of the sampled crystals need not necessarily be representative for the shapes of the halo-making crystals in the swarm. Our previous hypothesis [Appl. Opt. **33,** 4569 (1994)], that a spread of interfacial angles is the dominating cause of halo broadening, has proved untenable.

OCIS codes: 010.2940, 010.1290, 010.1110, 260.1440, 260.5430, 010.3920.

1. Introduction

In a previous paper[1] single-wavelength polarimetric parhelion and circumzenith arc observations with simultaneous crystal acrylic-spray replication of the halo-making crystals were presented. A mismatch of a factor 2.5 between the observed width of the halo peak in polarization and the width of this peak as calculated with the Fraunhofer diffraction theory from the observed size distribution of the replicated crystals was reported. This discrepancy was attributed to variability in the interfacial angles of crystals, if these crystals are growing while they fall. A variability of ~0.3° suffices to explain the observed width of the peak. Observational evidence was presented that the interfacial angles of sampled ice crystals were indeed not always exact multiples of 60°.

To collect more evidence about the proposed explanation, additional Antarctic fieldwork was carried out. This took place in the austral summer 1997–1998 at the U.S. Amundsen–Scott South Pole station. As before,[1] the first author of the present paper (Können) performed the fieldwork. The difference with the previous[1] (1990) experiments was that the polarimetry was now at two wavelengths (435 and 615 nm). Wavelength dependence of the halo birefringence peak provides information about the relative contribution of Fraunhofer diffraction to halo broadening, since Fraunhofer diffraction broadening of the halo's radiance and polarization is wavelength dependent, whereas broadening by other mechanisms (solar smearing, imperfect crystal orientation, and broadening resulting from variability in interfacial crystal angles) is not.

2. Theory

The theory of halo polarization by birefringence has been extensively presented[1,2] and is discussed only schematically here.

Halos generated by weakly birefringent crystals such as ice give rise to a narrow peak in polarization at the inner edge of the radiance distribution. This peak is called the birefringence peak (Fig. 1). For parhelia, this birefringence peak occurs in the second Stokes parameter Q if the reference direction for the Stokes parameters is the vertical. The polarization in the birefringence peak is in addition to the "normal" polarization that results from Fresnel losses at refraction; Ref. 1 describes the separation of these two components. The width of 0.1° of this peak in

G. P. Können (konnen@knmi.nl) and H. R. A. Wessels are with the Royal Netherlands Meteorological Institute, P.O. Box 201, 3730 AE De Bilt, The Netherlands. J. Tinbergen is with the University of Leiden and the Netherlands Foundation for Research in Astronomy, P.O. Box 2, 7990 AA Dwingeloo, The Netherlands.

Received 19 November 2001; revised manuscript received 1 April 2002.

0003-6935/03/030309-09$15.00/0

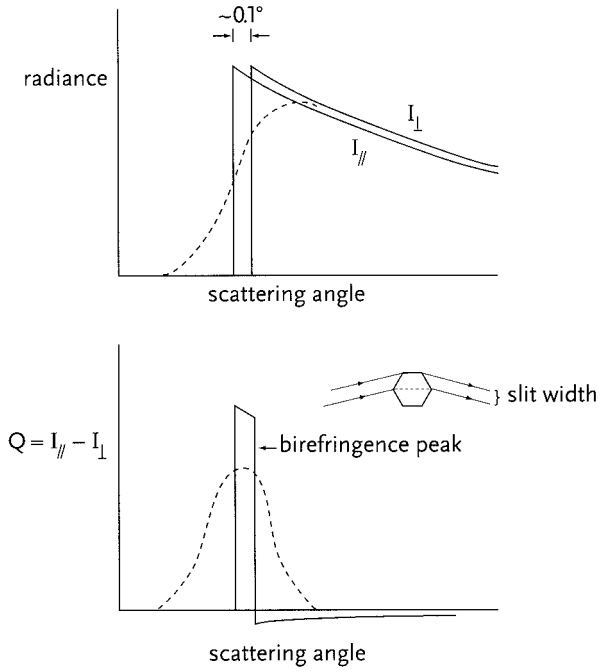

Fig. 1. Origin of the birefringence peak in parhelion polarization. Because of the polarization dependence of the refractive index of ice, the parhelion consists of two orthogonally polarized components, which are mutually shifted. For the 22° parhelion, the shift is ~0.1° in azimuth, and the component with horizontal polarization is closest to the Sun. Its radiance is denoted by $I_{//}$; that of the other component, by $I_{\perp}$. $Q = I_{//} - I_{\perp}$ is the second Stokes parameter. The solid curves give the two radiances $I_{//}$, $I_{\perp}$ and the Stokes parameter Q of the parhelion for the idealized situation of a point source located at infinity, perfect crystal orientation, no variability in interfacial crystal angles, and geometrical optics. The dashed curves show the broadening in a realistic situation. Among the broadening factors, only diffraction is strongly wavelength dependent.

idealized conditions (illumination by a point source located at infinity, perfect crystal orientation, no variability in the interfacial crystal angles, geometrical optics) is much less than in real life. The actual broadening is the same as that of the radiance distribution $I(\theta)$, i.e., determined by a convolution with a function $g(\theta)$. In this convolution integral the birefringence peak can be considered to be a δ-function so that

$$Q_{\text{birefr}} \propto g(\theta - \theta_h), \tag{1}$$

where Q_{birefr} is the birefringence peak and θ_h is the halo angle. The function $g(\theta)$ can be determined from the Fraunhofer diffraction function integrated over the size (slit width) distribution of the crystals and the other halo-broadening factors in the crystal swarm. Independently, Q_{birefr} can be determined from polarimetric observations. If all broadening factors are known, then these two determinations should lead to the same result.

Of the halo-broadening factors, only Fraunhofer diffraction is strongly wavelength dependent and size dependent. The Fraunhofer diffraction broadening function for crystals with constant aspect ratio is given by

$$g(\theta) \propto \sum_i d_i^4 (\sin x_i / x_i)^2 N(a_i) \Delta a,$$
$$x = \pi a \theta / \lambda, \qquad a = 0.38d, \tag{2}$$

where d is the crystal hexagon diameter (measured between opposite vertices), a is the slit width, λ is the wavelength, and $N(a)$ is the number of crystals per unit slit-width interval Δa.

The half-width at half-maximum (HWHM) of the birefringence peak Q_{birefr}, which according to Eq. (1) equals the HWHM of the broadening function $g(\theta)$, is defined by the difference in scattering angle between the maximum $g(0)$ and the half-maximum points $\frac{1}{2}g(0)$. The HWHM of the broadening function that results from diffraction alone is denoted by $\theta_{1/2}(\text{diff})$ and follows from relations (2). A Gaussian convolution rule may be used to decompose the value of HWHM as observed from the birefringence peak, $\theta_{1/2}(\text{obs})$, into a contribution by diffraction and a contribution that is due to other broadening mechanisms:

$$\theta_{1/2}{}^2(\text{obs}) = \theta_{1/2}{}^2(\text{diff}) + \theta_{1/2}{}^2(\text{others}). \tag{3}$$

3. Observations

A. Method

The observations took place at the U.S. Amundsen–Scott South Pole station. The observational approach was the same as before.[1] When a halo display appeared, pictures were taken with a camera equipped with a wide-angle lens (f = 7.5 or 16 mm). Crystal replicas were taken on a glass sheet of 5 × 5 cm, which was covered by a thin layer of liquid acrylic spray. This sheet was swept for ~15 s with a horizontal speed of ~1 m/s through the falling crystals surrounding us, some of which adhered to and submerged in the spray. After ~15 s the spray was hardened enough to collect no more crystals. Then the glass sheets were stored outside in the shade for 6 h to permit sublimation of the crystals, leaving their imprints as holes in the hardened spray. Typically, 500–1000 crystals were collected after a successful replicating. The glass sheets were taken home where the size distributions of the replicated crystals were determined. Parallel with the crystal replicating, crystal samples were collected for ~10 min in Petri dishes filled with hexane and then "live" photographed under a cooled microscope before they decayed. Usually a few tens of crystals are visible on each picture. The visibility of the halo in front of a nearby black object was verified, to ensure that the replicated and the sampled crystals were among those producing the halos.

Polarimetric pictures were taken with the rebuilt commercial four-lens camera described earlier.[1,2] The camera takes four images simultaneously on one Kodak Tri-X negative. The camera was mod-

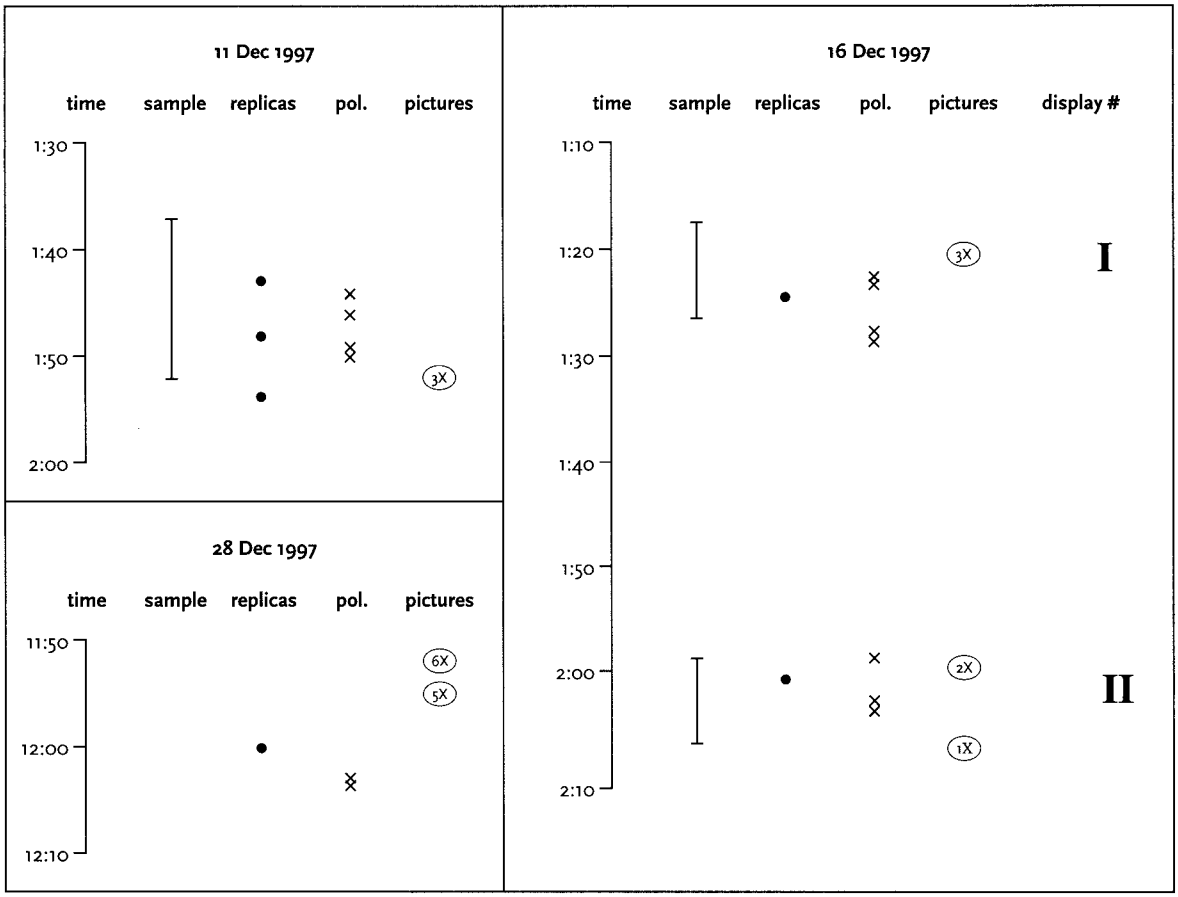

Fig. 2. Petri-dish crystal samplings, acrylic-spray crystal replicatings, polarimetric observations (pol.), and photographing sequences during the four 1997 South Pole displays. The time is South Pole local time (UT + 12 h).

ified with respect to the previous expeditions,[1] as it observed only one of the Stokes parameters (Q, U), but now at two wavelengths. Filters and emulsion define for the blue channel a passband of 30 nm centered at 435 nm; for the red channel the passband of 40 nm is centered at 615 nm. These passbands correspond to a 22° halo smearing of $\theta_{1/2} = 0.085°$ and 0.043° for the blue and the red channel, respectively. The negatives were digitized, and the photometric density was converted to radiance and then to polarization as described in Ref. 1.

The choice for a robust camera as polarimetric detector was made entirely on pragmatic grounds. Fieldwork experience in Antarctica has taught us that the scientific instruments have to be as reliable and as simple as possible in order to operate successfully in the harsh (−25 to −45 °C) Antarctic climate. For the present project, which aimed at documenting rarely occurring and usually short-lived phenomena, it is mandatory to have the observing instrument fully available at unpredictable moments. We are convinced that a more sophisticated instrument equipped with electronics and dependent on power supplies would have been less successful at collecting the data.

B. Data

On four occasions a successful set of observations was completed. All four sets included photography, crystal replication, and polarimetry; three of them were augmented with a meaningful crystal sample that was photographed under the microscope. In all cases, polarimetry was restricted to a parhelion. Figure 2 shows the sequences during the observations. The following details can be added:

16 Dec I and 16 Dec II Displays

These two unrelated events happened within 1 h. Both displays began at the end of an overcast situation, when the cloud cover gave way to clear sky. The way the clouds broke up reminded us of a frontal passage. This is in contrast to the 1990 event,[1] where the crystals seemed to originate from convective clouds. The Sun's elevation was 23°20′.

28 Dec Display

This display happened at the edge of an apparently old low-level fogbank, which was advected by the wind toward us. Contrary to the other displays, it is likely that the crystals were in equilibrium with the surrounding water vapor so that the growth rate of

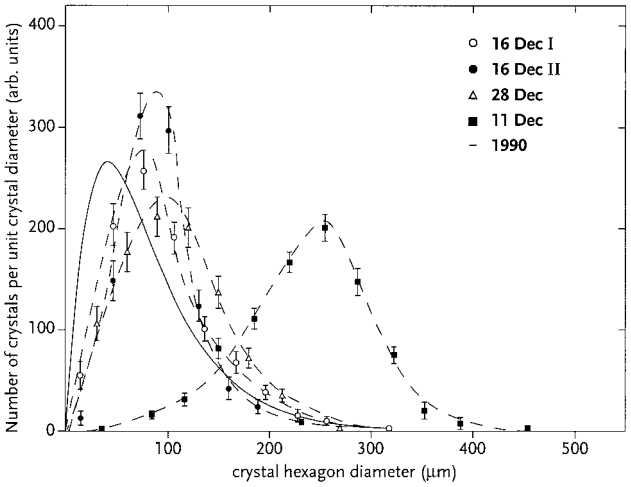

Fig. 3. Size distributions of the replicated crystals during the four 1997 South Pole displays. Only plate crystals were counted. The numbering of the 16 Dec displays is according to Fig. 2. The gamma distribution fit to the 1990 observation[1] is included as a solid curve. All distributions are normalized according to the number density in the acrylic-spray replicas.

the crystals would be close to zero. The Sun's elevation was 23°21′.

11 Dec Display

Like the two 16 December (hereafter, Dec) events, the 11 Dec display occurred in a frontal-passage-like situation. This display stands out from the other displays by the exceptionally large size of the sampled and the replicated crystals. Almost all crystals were thick plates. Crystals and display pictures looked very similar to those of the 4 January 1985 display, published as Figs. 1–15 and 1–16 in Tape's book.[3] The Sun's elevation was 23°01′.

Figures 3 and 4 contain linear and logarithmic plots of the observed size distributions of the plate crystals in the replicas. For the 11 Dec display, the graph was obtained from the sum over the three replica samples (Fig. 2). No difference was found between the size distributions in those three samples. Figure 5 shows the polarimetric observations of the 16 Dec II display. Similar data exist for the other days. The observed 435-nm values are multiplied by $I_{\max}(615)/I_{\max}(435)$ to account for differences in the film sensitivity and filter response between these wavelengths, where $I_{\max}(\lambda)$ is the maximum halo radiance at wavelength λ. For the 16 Dec II observation the shape of the halo anomaly in Q is close to that of the halo birefringence peak, Q_{birefr}. As expected, the widths of the peaks in Fig. 5 are inversely proportional to their peak values.

Table 1 shows the value of $\theta_{1/2}$(diff), calculated from the observed size distributions according to relations (2). Also in Table 1 are the observed values $\theta_{1/2}$(obs), as obtained from the polarimetric observations of the halo birefringence peaks. No reduction for solar smearing or camera passband smearing of the halo has been applied to $\theta_{1/2}$(obs), as this would result in a decrease of the values by only 0.03° or less. The experimental value of the 1990 $\lambda = 590$ nm observation[1] of $\theta_{1/2}$(obs) was multiplied by a factor of 615/590 before inclusion in Table 1, to account for the

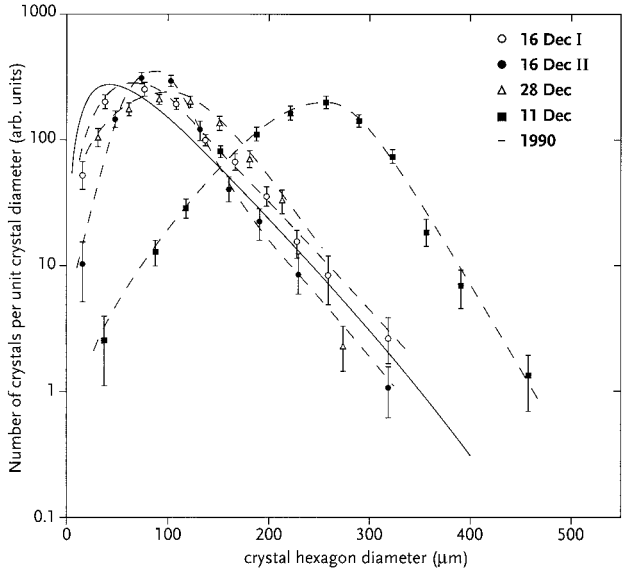

Fig. 4. Similar to Fig. 3; logarithmic scale for number density.

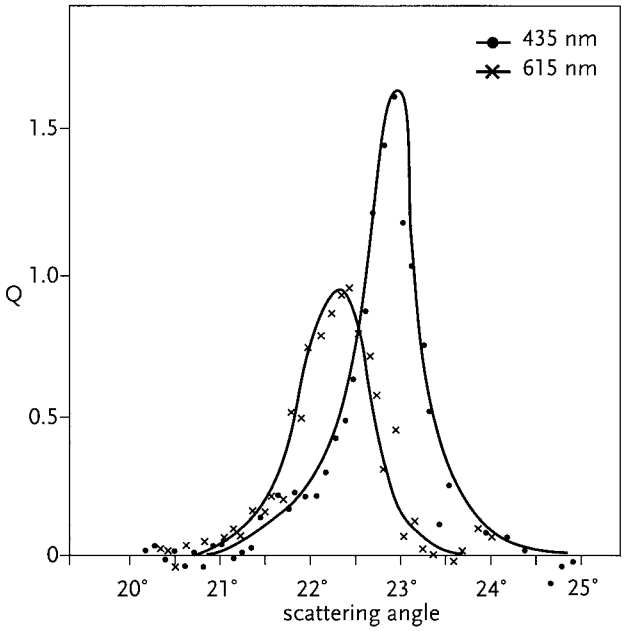

Fig. 5. Observed halo anomaly in the second Stokes parameter Q in the scan through the 16 Dec II parhelion. Arbitrary units. The intrinsic degrees of parhelion polarization at the maximum of the peaks are 10% and 16% for 615 and 435 nm, respectively. From the observational data the halo birefringence peak Q_{birefr} can be calculated.[1] The width of the birefringence peak relates to the size of the halo-generating crystals. Although in case of the 16 Dec II parhelion the shape of the anomaly in Q is close to that of Q_{birefr}, an accurate determination of the width $\theta_{1/2}$(obs) of the birefringence peak (Table 1) should be based on Q_{birefr} rather than straightforwardly on the shape of the halo anomaly in Q shown here.

Table 1. Half-Width at Half-Maximum Values $\theta_{1/2}$ of the Birefringence Peaks for the Two Wavelengths of Observation[a]

	λ = 435 nm		λ = 615 nm	
Display	$\theta_{1/2}$(diff)	$\theta_{1/2}$(obs)	$\theta_{1/2}$(diff)	$\theta_{1/2}$(obs)
16 Dec II	0.171 ± 0.007°	0.27 ± 0.02°	0.24 ± 0.01°	0.42 ± 0.02°
28 Dec	0.156 ± 0.007°	0.31 ± 0.04°	0.22 ± 0.01°	0.47 ± 0.05°
16 Dec I	0.139 ± 0.007°	0.51 ± 0.02°	0.20 ± 0.01°	0.70 ± 0.02°
11 Dec	0.098 ± 0.005°	0.39 ± 0.02°	0.14 ± 0.007°	0.52 ± 0.02°
1990	—	—	0.19 ± 0.01°	0.52 ± 0.02°[b]

[a] $\theta_{1/2}$(diff) is the value calculated from direct integration of the Fraunhofer diffraction function with the observed slit-width distribution of the plate crystals in the replica samples; $\theta_{1/2}$(obs) is the observed value from the polarimetry.
[b] Reduced from wavelength λ = 590 nm to 615 nm.

difference in observation wavelength. Figures 6 and 7 show the wavelength dependence of $\theta_{1/2}$(diff) and $\theta_{1/2}$(obs).

4. Interpretation

A. Wavelength Dependence of the Broadening

The width of the Fraunhofer diffraction peak in an ensemble of crystals is proportional to the size parameter:

$$\theta_{1/2}(\text{diff}) \propto \lambda/a_w, \tag{4}$$

where a_w is a size-distribution-weighted slit width. The wavelength ratio 615/435 in the polarimetric observations accounts in each display for a difference of a factor 1.41 in the width of the birefringence peak between the two wavelengths. The values $\theta_{1/2}$(diff) for a fixed wavelength of Table 1 indicate that the variation in a_w in our data should cause at each wavelength a maximal interdisplay variation in $\theta_{1/2}$(diff) of a factor 1.7. The largest interdisplay difference in $\theta_{1/2}$(diff) for a given wavelength is between the 16 Dec II and the 11 Dec displays. The large values of the interdisplay variation of $\theta_{1/2}$(diff) in our set of observations happen mainly by virtue of the exceptional size distribution in the 11 Dec replicated crystals (see Figs. 3 and 4).

As can be seen from Table 1 and Fig. 7, the dependence of $\theta_{1/2}$(obs) on wavelength is for each display in accordance with relation (4). Averaged over the four 1997 observations, $\theta_{1/2}$(obs, 615 nm)/$\theta_{1/2}$(obs, 435 nm) = 1.44 ± 0.05, in excellent agreement with the expected value of 1.41. The conclusion is that the broadening of the parhelion birefringence peaks should be attributed to diffraction. Other broadening mechanisms, including variability in interfacial crystal angles, have no detectable effect on the width of the birefringence peak.

B. Particle-Size Dependence of the Broadening

Comparison of $\theta_{1/2}$(diff) and $\theta_{1/2}$(obs) for a fixed wavelength in Table 1 reveal large discrepancies. First, $\theta_{1/2}$(obs) is on average a factor 2.5 larger than $\theta_{1/2}$(diff); second, there is no proportionality at all between $\theta_{1/2}$(diff) and $\theta_{1/2}$(obs). Given the conclusion of the previous paragraph that Fraunhofer diffraction determines the width of the parhelia, and given relation (4), such a proportionality should have

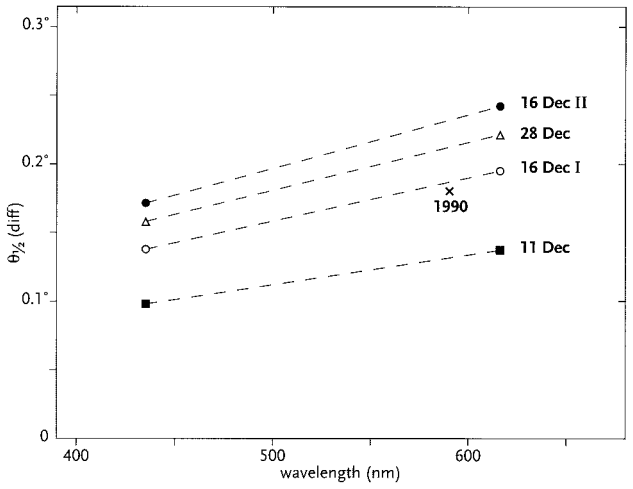

Fig. 6. Calculated half-width at half-maximum (HWHM) of the parhelion birefringence peaks $\theta_{1/2}$(diff), as obtained from direct integration of the Fraunhofer diffraction function with the observed slit-width distribution in the plate crystals from the replica samples (Fig. 4). Precise values of $\theta_{1/2}$(diff) are in Table 1.

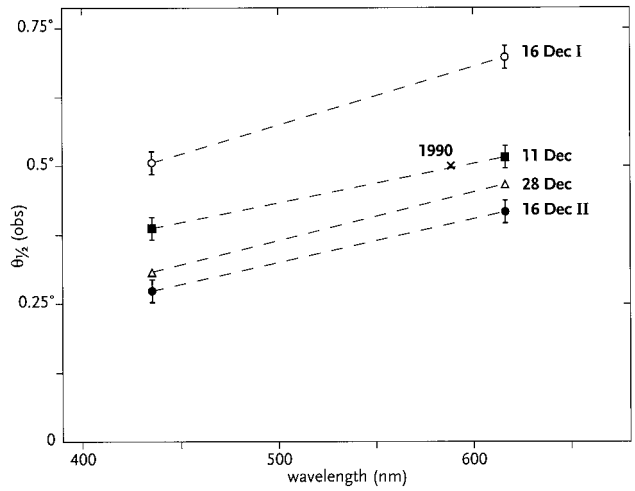

Fig. 7. Observed HWHM of the parhelion birefringence peaks $\theta_{1/2}$(obs). Note the difference in vertical scale with respect to Fig. 6 and the change in order of, e.g., the 16 Dec I and II displays with respect to Fig. 6. Precise values of $\theta_{1/2}$(obs) are in Table 1.

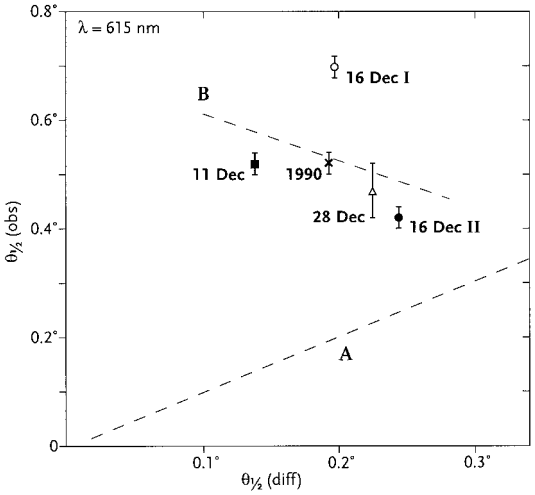

Fig. 8. HWHM of the birefringence peaks at $\lambda = 615$ nm. $\theta_{1/2}$(diff) is the value calculated from direct integration of the Fraunhofer diffraction function with the observed slit-width in the plate crystals from the replica samples; $\theta_{1/2}$(obs) is the observation from the birefringence peak. The 1990 observation is also included after reduction of $\theta_{1/2}$(obs) from $\lambda = 590$ nm to 615 nm. Precise values of $\theta_{1/2}$(diff) and $\theta_{1/2}$(obs) are in Table 1. Line A denotes the expected equality of $\theta_{1/2}$(diff) and $\theta_{1/2}$(obs). Line B is the observed relation, obtained from a least-squares fit; the correlation coefficient $\rho = -0.3$.

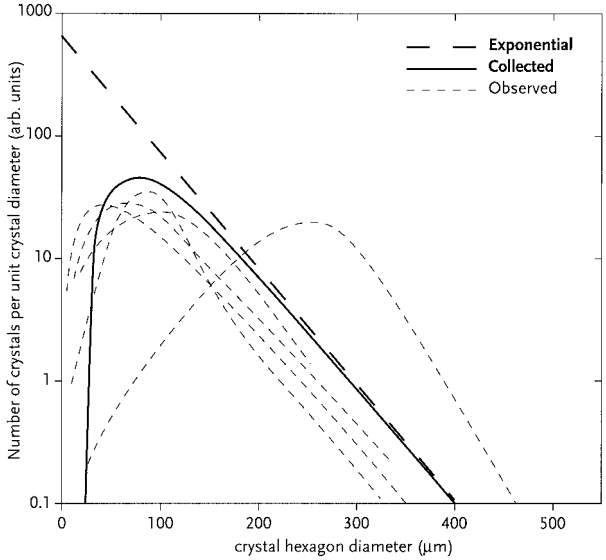

Fig. 9. Modification of a size distribution by the collection efficiency of the collector, according to Eqs. (5)–(8). Assumed is an exponential size distribution with average size 45 μm in the crystal cloud (bold, dashed). The bold solid curve is the size distribution of the crystals received by the collector assuming a wind speed of 4 m/s. The thin dashed curves are the actual observed crystal size distributions in our samplings (the curves of Fig. 4).

been observed. In Fig. 8 this point is further highlighted. Whereas $\theta_{1/2}$(diff) and $\theta_{1/2}$(obs) are expected to be the same for a given display, in Fig. 8 they are only weakly correlated. Contrary to expectation, the correlation coefficient ρ between $\theta_{1/2}$(diff) and $\theta_{1/2}$(obs) is even negative ($\rho = -0.3$).

This disagreement leads to the somewhat surprising conclusion that the size distribution in the replicated crystals is not representative for the size distribution of the halo-making crystals in the clouds.

C. Collection Efficiency of Crystal Replicating

In crystal replicating in still air, the number of small crystals is underestimated, because they are swept aside from the crystal-collecting glass sheet during the sweep in the process of sampling. The same underestimation occurs if the wind is blowing around a collector that is fixed, such as a Petri dish. Small particles are apt to follow the streamlines of the airflow and may miss the collector; big particles will collide with it. The effect, which is notorious in rain gauges, is often larger than intuitively thought.

The collection efficiency E_{col} is given by[4]

$$E_{\mathrm{col}} = CE, \tag{5}$$

where C is the coalescence efficiency and E the collision efficiency. For a first-order estimation of the collection efficiency of our spray-covered glass sheets that caught the crystals, the Langmuir theory, which is presented in Langmuir's article about rain formation,[5] is suitable.[4] The Langmuir collision efficiency E_L for spherical detectors and Reynold numbers $\gg 60$ is given by

$$\begin{aligned} E_L &= 0 && \text{if } K \le 1/12, \\ E_L &= 1/(1 + 0.5/K)^2 && \text{if } K > 1/12, \end{aligned} \tag{6}$$

where K equals the stopping distance divided by the radius of a cylindrical or spherical collector. K is given by[4]

$$K = \frac{2}{9}\,\rho v r^2/(R\mu), \tag{7}$$

where v is the velocity of the collecting detector with respect to the air, R is the radius of the collector, r the radius of the collected particle, $\mu = 1.6\ 10^{-5}$ Ns/m^2 the dynamic viscosity of the air at South Pole circumstances (air pressure 700 hPa, temperature −30 °C), and ρ the density of the collected particles. Assuming 100% coalescence efficiency C, E_L equals the Langmuir collection coefficient of the detector.

Under our replicating conditions R could be as large as the radius of the sleeve of our parka (0.1 m) rather than of order of the semidiameter of the crystal-collecting glass sheet (0.025 m) in our hand. Then Eq. (7) becomes

$$K = 32 v d^2, \tag{8}$$

where the particle diameter d is in mm and v is the velocity in m/s.

The typical wind speed at the South Pole and hence v is 4 m/s. Then, according to Eqs. (6), ice crystals with diameters smaller than ~25 μm escape repli-

cating; at $d \approx 50$, 100, and 150 μm, the collection coefficients E_L are 15%, 52%, and 73%, respectively.

The effect of the collection efficiency on the size distribution is illustrated in Fig. 9. Assuming an exponential distribution in the crystal sizes in the air results in a crystal size distribution in the replica that is peaked and will resemble a gamma distribution. The width of the birefringence peak $\theta_{1/2}$ as calculated from the modified distribution is in this example a factor of 1.5 smaller than it should be.

Even if the collection efficiency as a function of crystal size were exactly known, it is clear from Fig. 9 that it is almost impossible to reconstruct the real size distribution from the sampled ones. In reality the situation is worse, as Fig. 8 seems to indicate that the efficiency with which the halo-making crystals were collected varied from one display to another. This is an indication that the size dependency of the collection efficiency may be an important, but not the only, factor for why the halo-making crystals escape collection (see Subsection 5.C).

We conclude that in our experimental conditions many small crystals escaped collection, whereas they produce the dominant contribution to the radiance of the halo. The efficiency with which the halo-making crystals were collected varied erratically from one display to the next.

5. Discussion

A. Variability in Interfacial Crystal Angles

The analysis shows that our earlier hypothesis[1] that variability in interfacial angles of growing crystals is the dominating factor for halo broadening is not tenable. First, the dependence of the width of the birefringence peak on wavelength undermines this explanation; second, the fact that the experimental data from the 28 Dec display were similar to the others, although the crystal growth rate was apparently close to zero, is inconsistent with this explanation.

The above arguments do not mean that the hypothesis of variability of interfacial crystal angles should be completely dropped. There is still observational evidence[1,6] in sampled and replicated crystals that variability in interfacial angles does occur in growing crystals. However, the value of the mean variability $\delta_{1/2}$ should at most be half the previously[1] reported value of 0.3°, which was obtained under the assumption of a predominant contribution of this variability to halo broadening.

B. Broadened Halos and (Im)perfection of Crystal Orientations

The data show clearly that the parhelia are smeared out and that the smearing results from Fraunhofer diffraction. This broadening seems a common feature in Antarctic halos and is apparent in other quantitative observations, too.[7] Compared with mid-latitudes, even the bright halos and arcs are always of a somewhat diffuse appearance. This happens even in displays containing halos such as the Wegener arcs and the subhelic arc, which occur only when the crystal orientation in the swarm is almost perfect. The fact that the smearing stems from a process unrelated to the imperfection of crystal orientation explains the observational paradox of the presence of such exceptional halos in bright and still diffuse-looking Antarctic displays.

Although in mid-latitudes sometimes large and diffuse diffraction-broadened parhelia do sometimes occur, most mid-latitude parhelia and arcs are sharply defined. This means that the mid-latitude halo-generating crystals are usually of greater size than those of the Antarctic halos. The width of the birefringence peak of the typical mid-latitude parhelion observed earlier[2] was indeed of the order of the width of the Sun. The apparent small Fraunhofer diffraction smearing implies crystal sizes at least a factor of 3 larger than for our Antarctic parhelia.

It may be that 22° circular halos are an exception among the mid-latitude halos in the sense that the governing cause of their broadening is still diffraction. According to our 1998 multiwavelength polarimetric observation of a 22° circular halo with the aid of an astronomical telescope at La Palma,[2] the halo was diffraction broadened with $\theta_{1/2}(\text{obs}) = 0.8°$ at $\lambda = 622$ nm. If the La Palma halo is typical of mid-latitude 22° circular halos, this observation is consistent with the idea that smaller crystals are apt to be disoriented.[8] On the other hand, it should be noted that, for Antarctic halos, we failed to observe[1] in the 1990 display any significant difference in width between the birefringence peaks of the parhelion and the 22° circular halo. This seems to indicate that, for sizes of the order of the Antarctic halo-making crystals (~25 μm), the crystal (dis)orientation process is hardly dependent on crystal size. It is unclear which factors govern the disorientation process in this size range.

C. Undersampling of Halo-Making Crystals

The agreement of the wavelength dependency of the width of the birefringence peak with Fraunhofer diffraction for each display (Fig. 7), combined with the disagreement between observed widths in the various replica samples and the values calculated from direct integration of the Fraunhofer diffraction function with the observed slit widths (Fig. 8), suggests that the relation between replicated crystals and halo makers is weak. We attribute this nonrepresentativity primarily to size-dependent collection efficiencies in the replicating process. Although the possibility of an underestimation of the amount of small particles was considered in our earlier study,[1] we seem to have greatly underestimated its magnitude.

Consistency between the optical data and the crystal size distribution in the replica samples can be achieved only if a huge amount of additional small particles are added to the samples. There is no experimental hint whatsoever how the sizes of these "invisible" crystals are distributed. This leads to the conclusion that halo polarimetry (or even photome-

try), rather than our present method of crystal sampling, is the more reliable method for collecting size information about the halo-making crystals.

It is uncertain whether the Langmuir theory with coalescence efficiency C unity can sufficiently account for the observed mismatch. Size dependency of the coalescence efficiency can stem from decay or sublimation of small crystals when they touch the surface of the acrylic spay, or from a less-efficient penetration of small crystals through the surface because of the surface tension. Effects such as these may enhance considerably the size dependence of the collection efficiency in comparison with Eqs. (6) but are difficult to quantify. The irreproducible interdisplay variability in collection efficiency in our sampling may be caused by a strong dependence of the coalescence controlling factors on temperature and other meteorological parameters. It is not possible to reconstruct the collection efficiencies during our fieldwork with any precision.

Despite the interdisplay variability in collection efficiency, there is mutual consistency of the size distributions in the three 11 Dec replica samples. Apparently within the experimental situation of this display, the undersampling of small particles is reproducible. Like in all other displays, the polarimetry indicates the presence of many small crystals in addition to the large ones in the replicas. Reconstruction of the actual size distribution of the halo-making crystals for this particular display inevitably results in a bimodal size distribution. This raises the question of whether size-dependent collection efficiency is the only mechanism causing the discrepancy. Rather, the observed stability of the collection coefficient seems to suggest that for this particular display the small particles resided at higher levels and were out of reach of the crystal collector.

However, it is difficult to accept that this explanation should apply to all Antarctic displays observed by us. As discussed earlier[1] the appearance of the halos in front of a nearby black object—the perspective effects in the halos and the dynamically moving streaks in the halos—caused by the passing of nearby wind-driven crystals contradicts this hypothesis. For the generic case we believe that the governing mechanism causing the undersampling of the halo-making crystals must be the size dependency of the collection coefficient.

D. Relation between Collected and Halo-Making Crystals

The question remains of how informative the sampled crystals are for interpreting halos. The fact that halo-making crystals are so seriously undersampled makes it impossible to link radiance or polarization distributions quantitatively with the observed crystal sizes. The undersampling also implies that shapes of the sampled crystals need not necessarily be representative for the shapes of the halo-making crystals in the swarm.

Nevertheless, we believe that some qualitative information about the shapes of the halo-making crystal may remain in the samples. The 11 Dec replicated crystals, which are predominantly exceptional big and thick plates, look very similar to the 4 January 1985 crystals collected in Petri dishes by Tape[3]; both the 11 Dec 1997 and the 4 January 1985 displays consisted of almost pure plate halos and look very similar. This suggests that there is a realistic hint from the replica that something exceptional was going on. But much further than such qualitative statements one cannot go. Firm conclusions would require an improved sampling and replicating technique.

There are no reasons to believe that the representativity of the crystals sampled in Petri dishes is better than when replicated in the spray, because at the South Pole the wind is always blowing. Indeed, the Petri-dish samples that we collected (Fig. 2) also contained few small crystals. The limitations on the sampling processes seriously undermines any attempt at quantitatively interpreting halo displays with the aid of replicated or sampled crystals.[1,3,9]

Avoiding the size-selective collection would in general be hard. In still conditions one may make use of an instrument that sucks air and crystals with a well-defined speed toward a collector. If the collecting speed is of order 1 m/s and the instrument diameter is 5 cm, then 50-μm particles are collected with a Langmuir collision efficiency of $\sim$50%. However, if the wind is blowing like at the South Pole, then the experimental conditions are more difficult. In this case one is readily faced with a difficulty in determining the size-dependent collection coefficient, because the detector, the arm that holds it, and the body of the person preferentially bends the smaller particles away from the collector.

Given the constraints dictated by Antarctic fieldwork, the following simple solution could be explored to the sampling problem: The collector plate could be fixed on a long thin rod, which would little affect the airflow around the collector plate. Then the collector should be swept around at a great speed in order to increase the Langmuir collision efficiency and to make the measurement independent of the environmental wind. A great and reproducible collection speed can also be attained with some low-tech mechanical device, e.g., linear movement of the collector along a rail after release of a spring or rotational movement with help of a sling or turntable. Back home, laboratory experiments should be undertaken to check whether the coalescence efficiency is lower than 1 and to investigate the collection efficiency of the low-tech mechanical device.

6. Conclusions

The following points summarize our conclusions:

- The widths of the halo birefringence peaks, and hence the broadening of Antarctic halos, are determined by Fraunhofer diffraction.
- Other broadening mechanisms, including variability in interfacial crystal angles, have no detectable effect on the width of the birefringence peak.

• Although our earlier hypotheses should be withdrawn that variability in interfacial crystal angles has a perceptual effect on the broadening of Antarctic halos, some observational evidence remains that variability in interfacial angles does occur in growing crystals.

• Diffraction-broadened parhelia and halo arcs are common in the Antarctic but rare in the mid-latitudes. With the exception of the 22° circular halo, the mid-latitude halo widths are usually determined by other factors, in particular by the angular width of the light source (the Sun).

• Because of the strong size dependence of the collection efficiency, the size distributions in the replicated and sampled crystals are not representative for the size distribution of the halo-making crystals in the clouds. Halo polarimetry and halo photometry are more-reliable methods to determine a nominal size of the halo-making crystals than actual crystal sampling.

• There is no guarantee that the shapes of the sampled crystals are representative for those of the halo-making crystals in the swarm. This undermines any attempt at quantitatively interpreting halo displays with the aid of information about shapes from replicated or sampled crystals.

• Bringing the size dependence under control requires use of a calibrated instrument. To be suitable for Antarctic fieldwork, the device should definitely be low tech. The replicating technique should be checked with laboratory experiments, preferably in a cold room.

Walter Tape performed the Petri-dish crystal-sampling experiments and kindly made its results available to our project. This research was supported by National Science Foundation grant DPP-8816515 and in part by the Antarctic Program of the Netherlands Organization for Scientific Research (NWO).

References

1. G. P. Können, S. H. Muller, and J. Tinbergen, "Halo polarization profiles and the interfacial angles of ice crystals," Appl. Opt. **33,** 4569–4579 (1994).
2. G. P. Können and J. Tinbergen, "Polarimetry of a 22° halo," Appl. Opt. **30,** 3382–3400 (1992).
3. W. Tape, *Atmospheric Halos*, Vol. 64 of Antarctic Research Series (American Geophysical Union, Washington, D.C., 1994).
4. B. J. Mason, *The Physics of Clouds* (Clarendon, Oxford, UK, 1971), pp. 567–580.
5. I. Langmuir, "The production of rain by a chain reaction in cumulus clouds at temperature above freezing," J. Met. **5,** 175–192 (1948).
6. J. Hallet, "Faceted snow crystals," J. Opt. Soc. Am. A **4,** 581–588 (1987), Plate I.
7. G. P. Können and J. Tinbergen, "Polarization structures in parhelic circles and in 120° parhelia," Appl. Opt. **37,** 1457–1464 (1998).
8. A. B. Fraser, "What size of ice crystals causes halos?" J. Opt. Soc. Am. **69,** 1112–1118 (1979).
9. W. Tape, "Some crystals that made halos," J. Opt. Soc. Am. **73,** 1641–1645 (1983).